ELSEVIER

Journal of Chromatography A, 948 (2002) 3–17

JOURNAL OF CHROMATOGRAPHY A

www.elsevier.com/locate/chroma

Mass transfer in rectangular chromatographic channels

H. Poppe*

University of Amsterdam, Institute of Technical Chemistry, Research Group Polymer Analysis, Nieuwe Achtergracht 166, 1018 WV Amsterdam, The Netherlands

Abstract

Rectangular channels are explored nowadays for use in chromatographic and electrophoretic separations, especially after the possibilities of micromachining have become available to separation scientist. Expressions for plate heights expected for such experiments with an infinite channel width has been given by Giddings, while Golay derived the effect of finite channel width for unretained components. However, it remains unclear how the classical equations for plate height for retained components should be modified when the effect of finite channel width is taken into account. Also, the application of electroosmotic propulsion of the mobile phase leads to a flow profile different from the Poiseuille-type profile assumed in the above treatments, and no equations seem to be available for this situation. In this work, these problems have been addressed by an approach involving numerical Fourier transforms. Expressions for the plate height contribution from mobile phase mass transfer as a function of characteristic length d_c (the height of the channel, or the diameter for open cylindrical systems, OT), mean mobile phase velocity, u_m, diffusion coefficient D_m, retention factor, k', and width-to-height ratio, φ, can always be written as: $H = d_c^2 u_m / D_m F(k', \varphi)$. For cylindrical open systems, $F(k', \varphi)$ equals $1/96\ (1 + 6k' + 11k'^2)/(1 + k')^2$, the well-known Golay equation. In the present work, this is taken as a reference point; results are cast in the form $F(k', n) = (A + Bk' + Ck'^2)/(1 + k')^2$, where A, B and C replace the factors 1/96, 6/96 and 11/96 of the Golay equation. Values of A, B and C are reported for various values of φ. This is done for a selection from the large variety of conditions that can be imagined: Coating on one, two or four walls of the channel, non-uniform or uniform coating, pressure-driven (Poiseuille-type) or electro-osmotically-driven flow, surface charge on one, two of four walls, etc. It is found that the effect of finite channel width is large for unretained solutes (plate height for a wide channel is nearly eight times larger than that predicted when the finite channel width is ignored), whereas the plate height increase with retention is in many cases influenced only slightly.

Keywords: Mass transfer; Dispersion; Rectangular channels; Plate height; Flow profiles

1. Introduction

Rectangular ducts are often used today in the exploration of the possibilities for micromachined devices for picoliter-scale high speed separation processes [1–3]. In most of these efforts, electrophoresis is applied as the separation principle, but also gas–liquid chromatography and liquid–solid chromatography, as well as micellar electrokinetic chromatography have been implemented.

In the most successful analytical separation systems, the ducts are cylindrical. Thus, in gas chromatography, this is virtually the only design in use today, although in the past, more complicated ones, such as micro-packed columns and whisker-coated open tubes have been explored. In HPLC cylindrical packed columns are standard, while some research activities have been devoted to open tubular wall-coated columns.

*Tel.: +32-205-256-540; fax: +31-205-256-638.
E-mail address: poppe@anal.chem.uva.nl (H. Poppe).

0021-9673/02/$ – see front matter
PII: S0021-9673(01)01372-3

The theory of dispersion in open cylindrical systems is well developed. In fact, numerous derivations of plate height equations have been reinvented several times over the years. Most of these theories make clear that from just the separation point of view, the cylindrical open system does not leave much room for improvement, plate height and permeability are about the best one can expect.

A consideration of rectangular ducts from a broad perspective may therefore well start with the question: ''What advantages over open cylindrical ('Capillary') systems are to be expected?''.

As a part of a ''total analytical system on a chip'' these advantages may be large: Micromachining allows to integrate injection, splitting, separation, reaction and detection components in one piece of equipment (chip) that, if we can believe the workers in this field, can be easily mass-produced for a low price. As we are not experts in this field, and bearing in mind Kolthoff's maxim, ''Theory guides, experiment decides'', we will not discuss this issue further here and wait for further experiments to prove this point. That is, even when it turns out that the rectangular duct is inferior from the separation point of view, there is still reason to pursue the goal of a ''laboratory on a chip'', in which a (possibly inferior) rectangular separation unit could play a role.

From the vantage point of just analytical separation, a comparison of the performance relative to cylindrical open systems may take into account three aspects: (1) efficiency, (2) separation time, and (3) sample capacity.

In our opinion, these three points summarize the most important, if not the only relevant, aspects in comparison of design of different geometry (i.e. assuming that phase and solute properties, isotherm linearity, etc. are the same).

For pressure driven (PD) systems, the first two performance aspects are well summarized in the ''separation impedance'', introduced by Knox and Bristow [4,5], the product of the permeability factor ϕ and square of the reduced plate height h:

$$\mathrm{SE} = h^2\,\phi \tag{1}$$

The value of SE for a particular column design tells us how expensive the generation of plates is in terms of time, via the relation:

$$t_0 = h^2 \phi N^2 \cdot \frac{\eta}{\Delta P} = \mathrm{SE}\, N^2 \cdot \frac{\eta}{\Delta P} \tag{2}$$

where h is, as said, the reduced plate height, H/d_c for an open cylindrical column, H/d_p for packed column: SE is the separation impedance; N is the required plate number; η is the viscosity of the mobile phase; and ΔP is the available pressure.

For cylindrical open systems the permeability factor is $1/32$, while the Golay equation [6] for the plate height is in reduced form:

$$h = \frac{2}{\nu} + \frac{1 + 6\,k' + 11\,k'^2}{96\,(1 + k')^2} \cdot \nu \tag{3}$$

where k' is the retention factor, and ν is the reduced velocity, equal to:

$$\nu = \frac{u_m\, d_c}{D_m} \tag{4}$$

u_m is the mean linear velocity of the mobile phase; d_c is the column diameter (or any characteristic dimension of the cross section).

Note that for the value of SE (predated by Golay's performance index [6]) it is unimportant which measure is taken for the characteristic length; taking the radius of the column rather than its diameter results in twice as large h-values and four times smaller ϕ values, but the SE value remains the same. The same concept has been used in LC [7]: there is actually no need to know the value of the characteristic length (particle diameter).

Note also that the second term in Eq. (3) is non-zero for unretained solutes ($k' = 0$). The term describes the effect of slow mass transfer, not only between the mobile and the stationary phase, but also between different regions in the mobile phase (wall region versus core region) with differing velocities, an effect first quantitatively described by Taylor [8]. In this contribution ''mass transfer'' and ''C-term'' are understood in this broad sense, thus including the effect of non-uniformity in the velocity.

With these relations, the situation with respect to optimization of cylindrical open systems is described. For translation into practical conditions, it remains to determine the column radius. This has to be done (see Ref. [5]) such that the reduced velocity obtained is close to the value $\nu_{\min}$ where the expres-

Table 1
Minimum values for h and SE for cylindrical open systems (OT) as a function of k'

	$k' = 0.0$	$h' = 1.0$	$h' = 3.0$	$h' = 10.0$
ν_{min}	13.9	6.5	5.1	4.5
h_{min}	0.29	0.61	0.78	0.89
SE_{min}	2.7	12.0	19.7	25.6

sion for h (Eq. (3)) has a minimum, while at the same time the maximum allowable pressure difference is obtained. Thus, the data in Table 1 are indicative of the performance of cylindrical open systems under optimized conditions.

As can be seen in the original work [5], the appropriate diameter of the column depends on N, but most importantly, decreases with the diffusion coefficient in the mobile phase, D_m, and with the allowable pressure drop ΔP. We note in passing that in the original work by Golay and other early pioneers, the diameter was chosen such that a pressure of about one bar values for ν were close to ν_{min}, which has remained more or less the standard for many years. Only relatively recently, the Eindhoven group [9] has strongly and convincingly advocated the use of smaller diameters, with larger pressure drops over the column, in order to significantly speed up separations, while retaining the high resolving power (N). Thus, higher speed is invariably connected with smaller dimensions, column diameter in this case.

In the latter work, the importance of the third performance factor, the sample capacity (3) turned out to be quite important. The diameters used in Ref. [9], in the range of 50–100 μm, are a factor of 3 to 10 smaller than the ones used originally in capillary GC, say 300–500 μm. The sample capacity is proportional to the cross-sectional area of the column. This already means that sample capacity goes down with the square of the diameter. Moreover, the plate height also has its influence, as shown in Refs. [10,11]. Since, with constant h, H is again proportional to d_c it follows that the sample capacity goes down with the third power of the column diameter. Indeed, in the work of the Eindhoven group, the really minute amount being eluted from the 50 μm columns could only be detected with reasonable signal-to-noise ratios after sophisticated improvements in the detection systems had been made.

This situation occurs in extreme form in attempts to develop open tubular liquid chromatography, OT-LC. In this technique, competitive speed of separation can only be obtained [12,13] with column diameters of 10 μm and preferably less. So far, only rather restricted techniques, such as laser induced fluorescence and single-wire electrochemical detection [14–17] have been shown to be adequate for detection in this extreme form of miniaturized separation.

This long introduction brings us to one central point of this contribution: With rectangular channels, one can enlarge the cross section, without unduly impairing the speed/efficiency, by enlarging one dimension (the width of the channel, b, while the speed is retained because of the small height a) of the channel.

Giddings and Myers [18] were the first to experimentally explore this concept in liquid chromatography. For an infinitely wide channel, with coating of stationary phase on one wall, the other wall being inert, in which edge effect at the end of the ''b-dimension'' can be neglected, the expression for the plate height is in reduced form:

$$h = \frac{2}{\nu} + \frac{1 + 9\,k' + 78\,k'^2}{105\,(1 + k')^2} \tag{5}$$

where d_c is replaced by the channel height, a, so that: $h - H/a$ and $\nu = u_m a/D_m$.

The permeability factor ϕ for such an infinitely wide channel is:

$$\phi = 12 \tag{6}$$

This leads to Table 2.

A more favourable situation is when the stationary phase is present on upper as well as lower wall; in that case the expression becomes [6,18]:

$$h = \frac{2}{\nu} + \frac{1 + 9\,k' + 25.5\,k'^2}{105\,(1 + k')^2} \cdot \nu \tag{7}$$

Table 2
Minimum values for h and SE for pressure drive with retentive layer on one wall and edge effects neglected, as a function of k'

	$k' = 0.0$	$h' = 1.0$	$h' = 3.0$	$h' = 10.0$
ν_{min}	14.5	3.1	2.1	1.8
h_{min}	0.27	1.29	1.86	2.23
SE_{min}	0.9	20.1	41.7	59.6

This leads to Table 3.

The comparison with cylindrical systems was made already in Golay's pioneering paper [6]. As can be seen, the minimum plate height and the separation impedance differ not too much between open cylindrical and rectangular systems; only the case with the stationary phase at one wall only is definitely less favourable.

1.1. Edge effects

However, it has been noted later [19,20] that the effect of finite width of the channel may be important. The expression for the corresponding plate height contribution can not be derived as a closed form expression. Golay [19] used a series of Cos and Sin terms to describe the velocity profile, while Cifuentes and Poppe used a series composed on Cosh and Cos expressions for that purpose. From there, with e.g. the mathematical technique described by Aris, one can arrive at numerical data for the plate height contribution as a function of width-to-height ratio, φ, and reduced velocity ν. As the dependence of ν is strictly proportional, this is conveniently expressed as a C-term increment, as a function of φ:

$$\Delta h_{edge} = \Delta C(k', \varphi)\nu \quad (8)$$

Work in Refs. [19,20] has shown that for *unretained* solutes the h-values can be nearly eight times larger than those predicted by equations such as Eqs. (5) and (6). Unfortunately, results for cases with retention do not seem to be available, except for work [21] in which no numerical, ready-to-use data were given. Therefore, we decided to investigate such cases.

The edge effects play a role in pressure drive chromatography, but similar effects will also occur in zone electrophoresis (ZE) and electrically driven chromatography (EDC). For both systems plug flow is normally assumed. However, in narrow channels such as employed in micromachined systems, double layer overlap may be of some importance. This will lead to non-uniformity in velocity and thus to a mass transfer contribution. Also, even with plug flow, depending on the distribution of the stationary phase, differing results can be obtained, as will be shown.

The aim of this work is to find numerical data on the C-term in rectangular channels. A variety of situations have(s) been considered. In the relatively simple case of pressure drive, the flow profile is uniquely determined by the width-to-height ratio, φ. However, the stationary phase can be distributed in various ways. Whereas, for cylindrical systems, it is reasonable to assume a uniform layer along the circumference, in rectangular channels one can imagine several cases, which one is appropriate will depend on the way the channel is fabricated and the way the layer is applied (coated before or after the channel has been formed, ''bonding'', dynamic or static coating, etc.). For pressure drive, these cases are coded as: PDBO: stationary phase on one ''long'' wall, ''bottom only''; PDBT: stationary phase on two ''long'' walls, ''bottom and top''; PDAL: stationary phase on all four walls, ''all''. These codes can be

Table 3
Minimum values for h and SE for pressure drive with retentive layer on two walls and edge effects neglected, as a function of k'

	$k' = 0.0$	$h' = 1.0$	$h' = 3.0$	$h' = 10.0$
ν_{min}	14.5	4.9	3.6	3.1
h_{min}	0.28	0.82	1.11	1.29
SE_{min}	0.9	8.1	14.7	20.0

combined with a number for φ: e.g. ''PDBO64'' for $\varphi = 64$. Each case described by such codes will give different results in the C-term expression.

In the case of electrodrive with plug flow, one has the same three cases for the coating. As for the flow profile, channels with dimensions smaller than 1 μm ($a = 1$ μm) are rarely used. For these the product κa, for a common ionic strength of 0.001 mol/l, has a value of 100 (in water), for which value plug flow is quite a reasonable approximation [22,23]. Thus, probably the most important cases are those with plug flow prevailing, coded ''PLBO'', ''PLBT'' and ''PLAL'', with ''PL'' referring to plug flow.

As soon as more complicated electro-osmotic situations are envisaged, the number of possibilities increases drastically, because the nature of each wall is not only important for the retentive effect, but also, as each wall may have a particular electrical surface charge, for the flow profile. In addition, the degree of overlap depends on the ratio of absolute dimensions of the channel to the Debye length in the electrolyte, $1/\kappa$. Even when restricting the number of assumed possibilities for each of these factors, one arrives at a multitude of cases. We treated only a small selection of these.

2. Theoretical and methods

The method used to arrive at the plate height contribution (in terms of a C-term contribution) is not much different from the approach used by e.g. Giddings [24], Aris [25,26] and Clifford [27]. However, as we found it difficult to translate their formalisms into a numerical framework, we devised a similar method that is described below.

The transport equation for the solute in the system is:

$$\frac{\mathrm{d}c}{\mathrm{d}t} = D_m \cdot \left(\frac{\mathrm{d}^2 c}{\mathrm{d}x^2} + \frac{\mathrm{d}^2 c}{\mathrm{d}y^2} + \frac{\mathrm{d}^2 c}{\mathrm{d}z^2} \right) - u_0(x, y) \cdot \frac{\mathrm{d}c}{\mathrm{d}x} \qquad (9)$$

where: c is the concentration of the solute; D_m is its diffusion coefficient; z is the coordinate in the direction of migration; x is the coordinate in the direction of the height of the channel, running from 0 to a; y is the coordinate is the direction of the width of the channel, running from 0 to b; t is the time; and $u_0(x, y)$ is the mobile phase velocity, assumed to be independent of z and t, while the x and y dependencies are give by the mode of propulsion of the liquid (pressure drive, plug flow, etc. The mean value of u_0 is given as u_m.

Boundary conditions are given at the edges, $x = 0$, $x = a$, $y = 0$, $y = b$. They either impose $\mathrm{d}c/\mathrm{d}x = 0$, when the wall is inert, or impose a value for $\mathrm{d}c/\mathrm{d}x$ given by the retention and the diffusion coefficient, such that the mass flow towards the stationary layer agrees with the retention. Generally, the second derivative with respect to z (the migration direction) is neglected. It corresponds to longitudinal diffusion and the corresponding h-contribution can be added later.

The general idea of the method used here is as follows. In zeroth order approximation, it is assumed that there is perfect equilibrium; the solute migrates, with velocity u_i imposed by its degree of retention, without dispersion; its zone of given shape and height retains these properties, it only moves (ideal and linear chromatography). For such a situation it holds $\mathrm{d}c/\mathrm{d}t = -u_i \ \mathrm{d}c/\mathrm{d}z$. The value of $\mathrm{d}c/\mathrm{d}t$ is positive in the leading edge of the peak, negative at the trailing end.

When the zone has travelled a sufficiently long distance and has become broad, the $\mathrm{d}c/\mathrm{d}z$ value will be the same over a long range. Taking $\mathrm{d}c/\mathrm{d}z$ as a constant, $\mathrm{d}c/\mathrm{d}t$ will be constant during some time. The assumption is that this time is long enough to make the system behave as if $\mathrm{d}c/\mathrm{d}t$ had been constant infinitely long.

For obtaining a first order approximation, Eq. (9), with $\mathrm{d}c/\mathrm{d}t$ and $\mathrm{d}c/\mathrm{d}z$ taken as constants, can be solved (with an undetermined additive constant), in agreement with the boundary conditions. One obtains a concentration distribution, $c^1(x, y)$, of which the curvature is determined by $\mathrm{d}c/\mathrm{d}t$ and thus by $\mathrm{d}c/\mathrm{d}z$.

The dispersive effect is then obtained as follows: The flux needed for ideal migration (zeroth order approximation) (''MUST'') is calculated as the product of u_i ($= u_m/(1 + k')$ and the total amount of material at position z, mobile phase part as well as stationary phase part. The mobile phase part is found by the double integral of $c^1(x, y)$ over the x, y-range. The stationary phase part can be found from the retention factor and the concentrations $c^1(x, y)$ at the edges, This value ''MUST'' is compared to the

actual flux present when the concentration is $c^1(x, y)$ (''IS''). This is found as the double integral of ($c^1(x, y)\ u_0(x, y)$) over the x, y-range (the stationary phase does not contribute as there is no mass transport there). The difference between ''IS'' and ''MUST'' appears to be proportional to dc/dz (the unknown additive constant mentioned above cancels). This additional flux is therefore clearly imposed by the non-equilibrium, brought about by the finite value of dc/dz. It therefore can be interpreted as a dispersion coefficient connected with slow mass transfer:

$$\mathrm{DC} = (\mathrm{IS}-\mathrm{MUST})/(dc/dz) \tag{10}$$

The dispersion coefficient DC is translated into a plate height contribution Δh:

$$\Delta h = \frac{2\,\mathrm{DC}}{u_m} \tag{11}$$

Although certainly no mathematical proof of the validity of this scheme is given above, it has been tested by symbolically deriving virtually all of the known plate height expressions, such as given by Golay [19], Aris [25,26], Giddings [24] for infinite-slit and cylindrical systems. Also, in the numerical scheme as used here these known expressions are reproduced with satisfactory accuracy (2%). For instance, artificially imposing a y-independent flow (profile $x - x^2$) reproduces the results given in Eqs. (5) and (7) with this accuracy.

2.1. Further details

In actual computations, use was made of dimensionless coordinates, x, y and t, replacing the ones in Eq. (9) (indicated from here by a prime).

The coordinate x runs from $x = 0$ to $x = 1$, with x being x'/a, where x' is the physical position from the lower wall and a is the channel height. The coordinate y runs from $y = 0$ to $y = \varphi$, with y being y'/a, and φ being b/a. The coordinate t runs from 0 to infinity, with t being $t' \cdot D_m/a^2$, where t' is the physical time (t is ''reduced time'').

Assume that the flow profile is given (further details on establishing the flow profile will follow below):

$$u(x, y) = \mathrm{Function}\,(x, y) \tag{12}$$

The differential material balance for the solute in the mobile phase is given by:

$$\frac{d^2c}{dx^2} + \frac{d^2c}{dy^2} + \frac{d^2c}{dz^2} - u(x, y) \cdot \frac{dc}{dz} = \frac{dc}{dt} \tag{13}$$

while the boundary conditions are:

$$\frac{dc}{dx} = J_{x=0} \quad \text{at} \quad x = 0 \tag{14a}$$

$$\frac{dc}{dx} = J_{x=1} \quad \text{at} \quad x = 1 \tag{14b}$$

$$\frac{dc}{dy} = J_{y=0} \quad \text{at} \quad y = 0 \tag{14c}$$

$$\frac{dy}{dx} = J_{y=\varphi} \quad \text{at} \quad y = \varphi \tag{14d}$$

For the J values see below.

The third term on the left-hand side describes longitudinal diffusion; it can be neglected in the derivation of the C-term, its effect can be added later (term $2/\nu$) to obtain the total plate height.

Simplification of Eq. (13) is obtained as follows: In the zeroth order approximation (perfect equilibrium, ideal chromatography) it holds:

$$c(x, y, z, t) \approx F_0(x, y, z - u_i t) \tag{15}$$

From this the derivative dc/dt can be expressed as:

$$\frac{dc}{dt} = -u_i \cdot \frac{dc}{dz} \tag{16}$$

with which Eq. (13) can be simplified into one with the variable t missing.

$$\frac{d^2c}{dx^2} + \frac{d^2c}{dy^2} + [u_i - u_0(x, y)] \cdot \frac{dc}{dz} = 0 \tag{17}$$

Taking dc/dz as a constant, as discussed above, a partial differential equation with c, x and y as variables remains. Its solution over the range of the rectangle is determined (apart from an additive arbitrary constant, which will be shown to be unimportant) when boundary conditions at the four sides enclosing the rectangle are known. These can be found by considering the total amount of material per unit z that moves per time unit into the (or, when negative, i.e. at the rear of the zone, out of the) stationary phase sitting at the walls. This amount, dM/dt, can be found as a function of dc/dz as:

$$\frac{dM}{dt} = A_m(u_i - u_m)\, dc/dz$$
$$= a\ b\ (u_i - u_m)\, dc/dz \quad (18)$$

where A_m is the area of the rectangle, $A_m = a\ b$, equal to the cross-sectional area of the mobile phase.

Depending on the distribution of the stationary phase, dM/dt corresponds to fluxes at the edges: e.g. when there is stationary phase only at the bottom edge ($x = 0$, case BO), it holds:

$$\frac{dM}{dt} = J_{x=0}\, a \rightarrow J_{x=0} = -b(u_i - u_m) \cdot \frac{dc}{dz} \quad (19)$$

while in that case:

$$J_{x=1} = J_{y=0} = J_{y=1} = 0$$

When more edges are coated, the dM/dt value has to be distributed over the coated edges, resulting in smaller absolute J values.

In this way, boundary conditions, Eq. (14), for Eq. (13) are found as expressions for the dc/dx and dc/dy values, respectively.

For the numerical work needed in the present case for the rectangular geometry, the techniques described in pp. 514–521 and 858–861 of Ref. [28] could be followed straightforwardly. These involve the use of a Cosine Transform, in which the boundary conditions where inserted as constants in the ''source terms''.

The results could always be expressed in the format of the Golay equation, i.e.:

$$h = \frac{f_0 + f_1 k' + f_2 k'^2}{N(1 + k')^2} \quad (20)$$

where h is H/a: f_0, f_1, f_2, N are constants, to be compared to the values in the Golay equation; $f_0 = 1$, $f_1 = 6$, $f_2 = 11$, $N = 96$.

2.2. Flow profiles

The flow profile is governed by the differential equation:

$$\eta \cdot \frac{d^2u}{dx^2} + \eta \cdot \frac{d^2u}{dy^2} = f(x, y) \quad (21)$$

where $f(x, y)$ stands for the driving force.

For pressure drive:

$f(x, y)$
$= dP/dz$ (pressure gradient, independent of x and y) (22)

For electrodrive:

$$f(x,y) = E\ \rho(x, y) \quad (23)$$

where E is the longitudinal electric field and $\rho(x, y)$ is the charge density, brought about by the presence of surface charge on one or more of the walls.

Provided the electrical potentials are so low that the linearized Poisson–Boltzmann equation can be used (<50 mV), the charge density in turn is equal to:

$$\rho(x,y) = \sum_{\text{all walls } k} \kappa\ \sigma_k\ e^{-\kappa\ a\ wk} \quad (24)$$

where: κ, is the Debije constant; k, is the index of a wall; σ_k, is the surface charge (C/m^2) on wall k; and w_k, is the distance from that wall, e.g. w for the bottom wall is x, for the top wall is $(a - x)$.

Deriving the flow profiles needed to solve Eq. (13) from Eq. (21) can be done in at least two ways. Most consistent would have been to use sine transform methods. However, the method used (for no clear reason) was to develop a series expansion of u, starting from the expression for an infinitely wide slit width; end effects neglected. For pressure drive this is:

$$u(x) = 1/6\ (x - x^2)\ a^2 \cdot \frac{1}{\eta} \cdot \frac{dP}{dz} \quad (25)$$

This expression satisfies the differential Eq. (21) and the boundary condition at $x = 0$ and $x = 1$ ($u = 0$), but not the boundary condition at $y = 0$ and $y = \varphi$. In order to force agreement with the latter, one can add to Eq. (25), in the usual way, e.g. described in Ref. [20], terms:

$A_j \cosh(j\ \pi\ y) \sin(j\ \pi\ x)$ with integer j running
from 1 to infinity, (26)

that affect neither Eq. (21) nor the boundary conditions at $x = 0$, $x = 1$, while the A_j's can be chosen such (one-dimensional Sine Transform) that agreement with the boundary conditions at $y = 0$, $y = \varphi$ is approached for increasing length of the series.

For electrodrive, this method leads to awkward

expressions, that nevertheless could be managed by the software. For some simple and some complicated cases, the results of the series method were compared to those obtained with a sine transform, with satisfactory results.

2.3. Numerical aspects

All calculations were done on a personal computer with Pentium processor with 32 Mb RAM, using Mathematica version 4.0 (Wolfram Research, Champaign, IL, USA).

The application of the mathematics was, as said, straightforward, except that sometimes the numerical capacity of the personal computer was strained. Preferable had been to take the number of data points in the x direction, n_x, (that is the n_y, in the y-direction, being φ times larger) so large the results were no longer affected by it within a level of, say, 0.1%. This turned out to be the case when n_x was between 20 and 50. However, we wanted to obtain results for n-values up to 256. With $n_x = 20$ this would lead to $20 \cdot (256 \cdot 20) = 102\,400$ data points that would have been passed to the Fourier transform procedure. This was either to time-consuming, or it caused a short-of-memory error. In most cases we therefore used an n_x value of 10, with less accurate results, but allowing to increase φ to 256. An accuracy of about 3% overall was considered satisfactory, in view of the fact that experimental data on dispersion seldom have this accuracy.

The tables list values with many more decimal places than are justified by the limited accuracy, resulting from the rough discretization chosen. These decimals are given in order to facilitate future comparison with numerical results obtained by us and others in a later stage.

3. Results

3.1. Pressure driven systems

Fig. 1 displays the flow profile as found for a rectangular channel with $\varphi = w/h$ equal to 4, displayed as a contour plot. This is the same result as obtained in Ref. [20].

Table 4 lists the data for the plate heights obtained with pressure drive and coating on the bottom and top wall.

The numbers for f_0 describe the dispersion in the absence of retention. These can be compared to those reported in Ref. [20], which were obtained in a more symbolic approach. The agreement is satisfactory ($\approx <1\%$): Table 2 in Ref. [20] gives for $\varphi = 32$ a value $\kappa_{\mathrm{Aris}} \approx 0.125$. As discussed in that text, it is reasonable to augment it by 0.019 for (roughly) taking the diffusion in the height direction into account, leading to 0.144. This value is for the dispersion coefficient, so it is two times smaller than the h-related values used here. Also, it includes the factor $1/105$. Finally, it was derived taking *half* the channel height as characteristic length, leading to a factor 4. Bringing the presently found f_0 factor on the

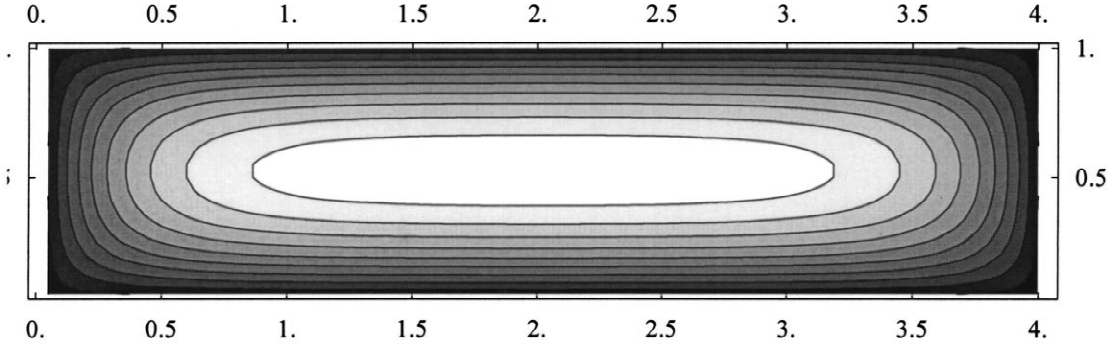

Fig. 1. Contour plot describing the flow profile under pressure drive in a rectangular channel with width over height ($\varphi = w/h$) equal to 4. Contours at 0.1, 0.2 . . . 0.9, 1.0 of the maximum flow velocity. Flow resistance factor ϕ for this n-value found as 14.244 (as compared to 32 for a cylindrical column, and 12 for an infinitely wide channel).

Table 4
Case PDBT: pressure drive, stationary phase at bottom and top walls

φ	f_0	f_1	f_2	ϕ
No edge effect	1.000	9.000	25.500	12.000
256.0	7.935	22.956	32.521	12.030
181.0	7.917	22.920	32.503	12.042
128.0	7.892	22.870	32.478	12.059
90.6	7.857	22.799	32.442	12.084
64.0	7.808	22.699	32.391	12.119
45.2	7.737	22.556	32.319	12.170
32.0	7.638	22.357	32.218	12.241
22.6	7.498	22.072	32.074	12.344
16.0	7.301	21.673	31.872	12.492
11.4	7.029	21.124	31.595	12.702
8.0	6.632	20.318	31.187	13.026
5.6	6.072	19.183	30.611	13.522
4.0	5.360	17.736	29.876	14.244
2.8	4.411	15.800	28.889	15.484
2.0	3.434	13.781	27.848	17.491
1.4	2.494	11.781	26.787	21.399
1.0	1.804	10.196	25.892	28.450

$n_x = 10$; $N = 105$; $h_{mt} = 1/105 \cdot (f_0 + f_1 k' + f_2 k'^2)/(1 + k')^2 \nu$.

same scale results in a value $(4/2)/105 \cdot 7.638 = 0.145$. The results also agree satisfactorily with the number 0.1514, given by Golay [19], for κ_{Aris}, again with half the channel height as characteristic length. Thus is should be divided by 4, and multiplied by 2 (for obtaining plate height) in a comparison with present data. This gives $f_0/N = 0.1514/2 = 0.757$, to be compared with Table 4, row $\varphi = 256$: $f_0/N = 7.595/105 = 0.756$.

The first line in Table 4 is given in order to facilitate a comparison with the results when edge effects are absent. It is seen (as demonstrated in Refs. [19,20]) that the edge effect for large φ-values increases the plate height for unretained solutes by nearly a factor of 8.

The numbers for f_0 in column two of Table 4 suggest also that for n-values larger than 8 the factor is essentially constant, and between 7.0 and 8.0. Indeed, it can be derived (not shown in this paper) that increasing φ further does NOT bring f_0 back to the ''no-edge-effect'' value of 1, it rather retains its value of about 7.5. This can be understood as follows:

With such large values for φ the system is uniform over a long range in the middle; only at the edges there is a region of smaller flow velocity (this is already visible in Fig. 1, for $\varphi = 4$). The volume fraction of this region decreases in proportion to φ. Its effect on the plate height, however, does not decrease, as it weight in the dispersion goes up with n. Apparently, these two counteracting effect cancel, so that the influence of the edge region on h finally becomes a constant.

It is possible to treat the situation as that of a retentive layer at the edges, with distribution coefficient 1. The gradual slowing down of the solute when it is closer to the edge is then replaced by a model where the velocity is zero within a distance δ from both edges, and has the full value in between these boundaries. δ is of the order of a (b is supposed to be much larger). The retention factor k'' is then $2\delta/(b - 2\delta)$. Neglecting all non-equilibrium in the x-direction, and using the expression for a one-dimensional duct of width b, uniform flow, retention on left and right side, one obtains:

$$h = 1/12\, b^2 (k'/(1 + k''))^2 \approx 1/12\, b^2\, k''^2 \approx 1/12\, b^2\, (2\,\delta/b)^2 = 1/3\,\delta^2 = \text{some constant}\, a^2 \quad (27)$$

indeed, independent of b.

The values of f_0 are of course independent of the mode of coating, so in all pressure drive systems discussed here they are the same. Therefore, in the discussions of following tables pertaining to pressure drive no attention will be given to f_0 any more.

The values of f_1 and f_2 describe the influence of retention. Although the values differ slightly from those in the top line (no edge effect), it can be seen that for this particular case (coating on bottom and top, i.e. inert left and right walls and pressure drive), the difference is not dramatic. The resulting differences in h would probably be of no importance at all in design considerations for analytical systems.

The bottom line in Table 1, describing a channel with square cross-section, is interesting, as this geometry is approaching the situation in the cylindrical system. Indeed, it is seen that f_0/N, f_1/N and f_2/N approach the values in the Golay expression, Eq. (3), within a factor of 2.5: Including the factors $1/96$ and 105 the comparison is between {0.0104, 0.0625, 0.115} and {0.0172, 0.0971, 0.275}.

Table 5 gives the results for coating at the bottom wall only. Striking is that the f_1-values are the same

Table 5
Case PDBO: pressure drive, stationary phase at bottom wall only

φ	f_0	f_1	f_2
No edge effect	1.000	9.000	78.000
256.0	7.935	22.956	85.021
181.0	7.917	22.920	85.003
128.0	7.892	22.870	84.978
90.6	7.857	22.799	84.942
64.0	7.808	22.699	84.891
45.2	7.737	22.556	84.819
32.0	7.638	22.357	84.718
22.6	7.498	22.072	84.574
16.0	7.301	21.673	84.372
11.4	7.029	21.124	84.095
8.0	6.632	20.318	83.687
5.6	6.072	19.183	83.111
4.0	5.360	17.736	82.376
2.8	4.411	15.800	81.389
2.0	3.434	13.781	80.348
1.4	2.494	11.781	79.287
1.0	1.804	10.196	78.392

$n_x = 10$; $N = 105$; $h_{mt} = 1/105 \cdot (f_0 + f_1 k' + f_2 k'^2)/(1 + k')^2 \nu$; φ values as in Table 4.

Table 6
Case PDAL: pressure drive, stationary phase at all walls

φ	f_0	f_1	f_2
No edge effect	1.000	n.a.	n.a
256.0	7.935	44.791	71.585
181.0	7.917	44.664	71.363
128.0	7.892	44.485	71.052
90.6	7.857	44.234	70.617
64.0	7.808	43.879	70.003
45.2	7.737	43.381	69.146
32.0	7.638	42.691	67.964
22.6	7.498	41.726	66.325
16.0	7.301	40.404	64.107
11.4	7.029	38.642	61.195
8.0	6.632	36.165	57.188
5.6	6.072	32.863	51.989
4.0	5.360	28.911	45.952
2.8	4.411	23.931	38.522
2.0	3.434	18.921	31.043
1.4	2.494	14.007	23.423
1.0	1.804	10.198	17.144

$n_x = 10$; $N = 105$; $h_{mt} = 1/105 \cdot (f_0 + f_1 k' + f_2 k'^2)/(1 + k')^2 \nu$; φ values as in Table 4.

as in Table 4. We do not have an explanation for this. The values for f_2, which determine the h-values at high retention, are about 2.5 times larger, a result of the larger distance over which equilibration by diffusion has to take place.

Again, the edge effect on f_2 is very small, ''no edge effects'' gives a value of 78 (analytical solution), whereas the other values in the table vary between 85 and 78.4.

As an illustration, Fig. 2 shows the concentration profiles obtained for this case with $\varphi = 4$ (PDBO4) and $k' = 3$

Table 6 list values for the case where the stationary phase is uniformly coated on all walls. The row ''No edge effect'' does not list f_1 and f_2 values, as the edge is here implicitly present.

Striking is the large increase of f_2 in comparison to Table 6 (all walls versus bottom and top, e.g. at $\varphi = 256$, 71.6 versus 32.5). This can be explained by the non-uniformity of stationary-phase; solutes close

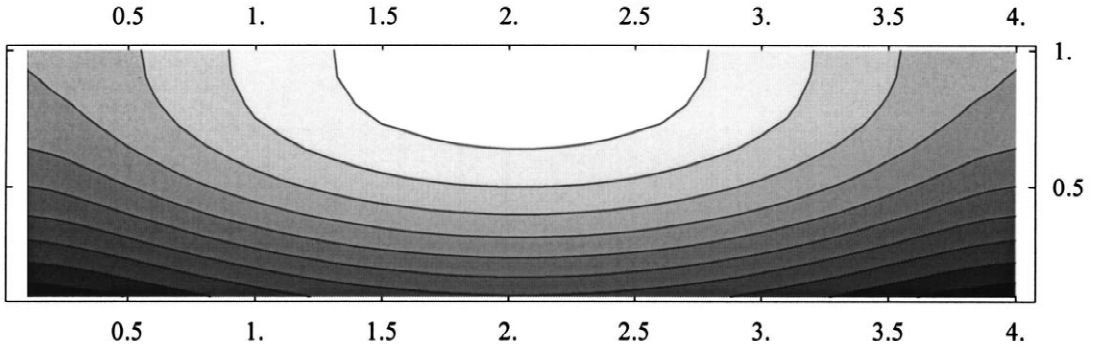

Fig. 2. Contour plot describing the concentration profile in the front of the peak ($dc/dz < 0$, $dc/dt > 0$). Pressure drive with stationary phase on bottom wall only; width-to-height ratio, $\varphi = 4$. Case ''PDBO4''. Retention factor, $k' = 3$. White corresponds to the highest concentration, black to the lowest.

to the edge ''see'' a more than average presence of the stationary phase, they will tend to migrate slower than the average, an effect than has to be counteracted by the cross-diffusion in the mobile phase over the width (which is large) of the channel. The difference in f_2 values between Tables 6 and 4 becomes smaller at smaller aspect ratios φ.

The data for the smallest n-value, in the last row, approach the values in the Golay equation better than was the case in Table 4. Including the N factors 96 and 105, and now multiplying the Golay factors by $4/\pi$, in order to have the same cross-sectional area, the comparison is between {0.0133, 0.0796, 0.146} and {0.0172, 0.0971, 0.163}.

3.2. Electro-drive systems with plug flow

In most discussions of dispersion in electro-driven systems plug flow is assumed, so that is also the main approach here. With such an assumption, the expression for the plate height contribution with coating on the bottom wall, and neglecting edge effect is:

$$h = \frac{4}{6} \cdot \frac{k'^2}{(1+k')^2} \cdot \nu \tag{28}$$

For coating on both bottom and top wall:

$$h = \frac{1}{6} \cdot \frac{k'^2}{(1+k')^2} \cdot \nu \tag{29}$$

so that, for these two cases, $f_2/N = 1/6$, $f_2/N = 4/6$, respectively, while f_0 and f_i are zero [24].

As explained in Section 1, four modes of stationary phase coating are considered mainly. However, for plug flow, with the coating modes ''bottom and top'' and ''bottom only'' only trivial results are obtained, as the analytical solutions, Eqs. (28) and (29) apply. These cases have been some of the opportunities for validation of the numerical scheme used, and therefore some results are shown in Table 7. As can be seen, the data exactly agree with Eq. (28). The values for f_0 and f_1 are all zero.

Table 8 shows non-trivial results for coating on all walls. Again, the results for f_0 and f_1 are all zero, therefore these are not included in the table.

As can be seen, the f_2 value goes up with n; for $\varphi = 1$ (square channel) the value is 0.5, going up to 1.984 for $\varphi = 256$. A similar effect as noticed for f_0 in the pressure driven case occurs here: The value of f_2 appears to approach a constant value when φ becomes very large. A reasoning similar to that given in the discussion of Table 4 may be given to explain this: At the left and right edges the migration velocity is smaller as there is more stationary phase ''visible'' from each liquid element. For design consideration, it important to note that a very wide channel with coating on four walls has, for large k', a nearly four times larger plate height than a square channel of the same height, a.

We note in passing that the value of nearly exactly 0.5 for the square channel (bottom row of Table 8) suggest that an analytical solution for this case must exist. We have no idea what this is.

Table 7
Case PLBO; plug flow, stationary phase on bottom wall only

φ	f_0	f_1	f_2
No edge effect	0	0	4.000
4.0	0	0	4.000
2.8	0	0	4.000
2.0	0	0	4.000
1.4	0	0	4.000
1.0	0	0	4.000

$n_x = 10$; $N = 6$; $h_{mt} = 1/6 \cdot (f_0 + f_1 k' + f_2 k'^2)/(1+k')^2 \nu$.

Table 8
Case PLAL: plug flow, stationary phase on all walls

φ	f_2
No edge effect	n.a.
256.0	1.984
181.0	1.978
128.0	1.969
90.0	1.957
64.0	1.939
45.2	1.914
32.0	1.881
22.6	1.834
16.0	1.772
11.4	1.690
8.0	1.580
5.6	1.440
4.0	1.280
2.8	1.086
2.0	0.889
1.4	0.681
1.0	0.500

$n_x = 10$; $N = 6$; $h_{mt} = 1/6 \cdot (f_0 + f_1 k' + f_2 k'^2)/(1+k')^2 \nu$.

3.3. Electro-driven systems with double layer overlap

It is not certain if ever double layer overlap may be of importance in open channels. As follows, from the work by Rice and Whitehead [22] and Knox and Grant [23], double layer overlap does not affect the mean flow velocity when:

$$\kappa a \approx > 20 \quad (30)$$

where κ is the Debije constant (inverse of the Debije length); a, is the diameter of the cylindrical channel, or a characteristic length of the duct, in our case indeed the ''a'', the height of the channel.

Although this was derived for cylindrical channels, the situation for rectangulars will not be much different. With usual values of the ionic strength, this corresponds to a-values below 1 μm. Thus, it seems unlikely that ever these cases are of importance for rectangular channels.

Nevertheless, for several reasons, we decided to include double layer overlap in our study. First, ducts of 1 μm height have already been used for separation purposes [29,30]. Second, one may try, e.g. in view of heat dissipation, to work at lower ionic strength, where overlap is more likely. Third, the κa value of 20 in Eq. (24) pertains to the onset of appreciable decrease in flow velocity; but it could be that the increase in h-contribution due to non-uniform flow at the walls begins earlier.

3.4. Surface charge on all walls

Fig. 3 shows the flow profile for a channel with $\varphi = 4$, with surface charge on all walls and κa equal to 10. The flow reduction as a result of double layer overlap is at these values of κa and φ equal to 0.781.

The profile has a peculiar shape. Near the left and right end there are regions where the velocity is larger than in the centre of the channel. Physically this is understandable: The driving force resides close to the wall, where the double layer sits. A liquid elements near both ends experience driving forces originating from three walls, whereas in the middle only two walls contribute to the propulsion of the liquid.

It is noteworthy that in an early paper by Golay [19], it was proposed to generate a similar profile (i.e. larger velocities near the left and right end) in order to ameliorate the plate height increase due to non-uniformity in the y-direction (see discussion above following Eq. (8)). That is, the long-range influence of the stagnant part near the left and right walls was to be compensated by a higher velocity close to that wall. Golay envisaged to realize this by making the channel height somewhat larger at the end; in the present case of electrodrive this ''Golay effect'' is realized by the presence of electro-osmotic propulsion at the vertical walls.

Table 9 lists the f values for this case, again for

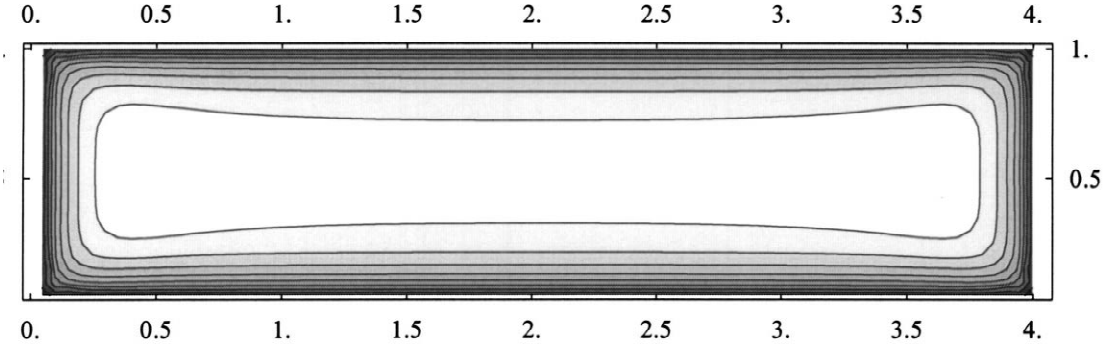

Fig. 3. Contour plot describing the flow profile under electro-driven conditions in a rectangular channel with width over height ($\varphi = w/h$) equal to 4; $\kappa a = 10$. Surface charge on all walls assumed equal. Contours at 0.1, 0.2 . . . 0.9, 1.0 of the maximum flow velocity. Flow reduction factor (compared to infinitely wide channel with same surface charge) 0.781.

Table 9
Electro-driven with $\kappa\ a = 10$: surface charge on all walls; stationary phase on all walls

φ	f_0	f_1	f_2
No edge effect	0.000	0.000	n.a.
256.0	0.029	0.495	2.451
181.0	0.029	0.495	2.444
128.0	0.029	0.495	2.435
90.6	0.029	0.494	2.422
64.0	0.029	0.494	2.404
45.2	0.029	0.493	2.378
32.0	0.030	0.492	2.343
22.6	0.030	0.490	2.294
16.0	0.030	0.487	2.228
11.4	0.031	0.483	2.143
8.0	0.032	0.478	2.026
5.6	0.033	0.469	1.876
4.0	0.034	0.457	1.702
2.8	0.036	0.436	1.487
2.0	0.037	0.407	1.259
1.4	0.037	0.362	1.006
1.0	0.035	0.305	0.771

$n_x = 10;\ N = 6;\ h_{mt} = 1/6 \cdot (f_0 + f_1 k' + f_2 k'^2)/(1 + k')^2 \nu.$

Table 10
Electro-driven with $\kappa\ a = 10$: surface charge on bottom and top walls; stationary phase on bottom and top walls

φ	f_1	f_2	f_2
No edge effect	0.000	0.000	1.000
256.0	0.379	1.018	1.639
181.0	0.378	1.016	1.638
128.0	0.377	1.013	1.636
90.6	0.375	1.009	1.634
64.0	0.373	1.004	1.631
45.2	0.369	0.996	1.627
32.0	0.363	0.984	1.621
22.6	0.356	0.968	1.612
16.0	0.345	0.945	1.600
11.4	0.331	0.914	1.583
8.0	0.309	0.868	1.559
5.6	0.279	0.803	1.524
4.0	0.241	0.719	1.478
2.8	0.190	0.605	1.415
2.0	0.137	0.480	1.343
1.4	0.086	0.342	1.256
1.0	0.049	0.209	1.160

$n_x = 10;\ N = 6;\ h_{mt} = 1/6 \cdot (f_0 + f_1 k' + f_2 k'^2)/(1 + k')^2 \nu.$

various values of φ. The small f_0 values are noteworthy; they are close of 0.03 for large φ values, which is 30 times smaller than the value for a pressure drive system (see also discussion of Table 10 below, where the improvement in h is much smaller).

As can be seen, the f_2 values become essentially constant when the width-to-height ratio, φ, exceeds 16. These values lead to plate heights h that about a factor of 2.5 larger than those predicted by Eq.. (29), i.e. $f_0 = f_1 = 0$ and $f_2 = 1$. Taking the latter as a reference value: The higher values for f_2 at large φ must be attributed to the non-uniformity of stationary phase ''visibility''; the decrease when φ approaches 1 is explained by the presence of stationary phase at h vertical walls; the system is roughly approaching the cylindrical system.

Table 10 applies to the case in which the left and right walls are entirely inert, from the point of view of retention as well as that of electroosmosis. They thus act only as a source of friction, impeding the liquid movement.

The data for f_0 may be compared to those of Table 9 (where the Golay effect was present). Although the f_0 value for pressure drive (1) is not reached, the non-uniformity of flow results in an increase of f_0 from 0.03 (Table 9, high n) to 0.38 (Table 10, high φ).

3.5. Special case with double layer overlap

As a special case the following was studied: Electro-osmotic activity on top, left and right wall; retentive activity only on the bottom wall, which is electroosmotically inactive. This case may be approached in practice in a system made of quartz or silicon with an oxidized surface layer (SiO_2). When the cover plate has been silanized externally before bonding, it would acquire a retentive function, but may loose the electro-osmotic activity. The velocity near the retentive wall is smaller than elsewhere in the cross-section. The results for this case, again for a value of $\kappa\ a$ of 10.0, are listed in Table 11.

The f_0 values (0.103–0.329) are similar (but not the same, IX:0.029–0.037, X:0.379–0.49) as in Table 10; there being a difference in the flow profile as the left and right walls now contribute to the propulsion of the liquid. Surprisingly, the ''Golay effect'', which was invoked above to explain the

Table 11
Electro-drive with $\kappa a = 10$: surface charge on left, right and top wall; stationary phase on bottom wall only

φ	f_0	f_1	f_2
No edge effect	0.000	0.000	4.000
256.0	0.329	2.168	5.840
181.0	0.327	2.164	5.837
128.0	0.325	2.159	5.833
90.6	0.322	2.150	5.828
64.0	0.318	2.139	5.821
45.0	0.313	2.123	5.810
32.0	0.306	2.101	5.796
22.6	0.295	2.071	5.775
16.0	0.282	2.029	5.748
11.4	0.264	1.975	5.711
8.0	0.240	1.901	5.660
5.6	0.211	1.805	5.594
4.0	0.181	1.696	5.515
2.8	0.151	1.567	5.416
2.0	0.130	1.440	5.311
1.4	0.115	1.304	5.189
1.0	0.103	1.167	5.065

$n_x = 10$; $N = 6$; $h_{mt} = 1/6 \cdot (f_0 + f_1 k' + f_2 k'^2)/(1 + k')^2 \nu$.

difference between the propulsion at top and bottom on one hand and that by all walls on the other hand, does not lead here to small f_0 values. Apparently, the increase in velocity when approaching the left and right wall is too strong in relation to the propulsion by only the top wall. Indeed, in a separate experiment (not shown), where the electro-osmotic activity at left and right walls was reduced by a factor 2, the results for f_0 were much lower.

As the fastest flow lines are relatively far away from the retentive layer, one would expect an large h-contribution for high retention. That is indeed what is obtained, the f_2-values varying between 5.065 and 5.840, whereas plug flow leads to $f_2 = 4$.

4. Discussion

Although a large amount of data has been produced, the main trends can be summarized briefly:

In pressure drive systems the most significant effect is that on unretained components: With large width-to-height ratios the f_0-values approach a limiting value close to 8, that is, the h-contribution is nearly eight times larger than is expected when edge effects are neglected (Eqs. (5) and (7)). With no stationary phase on the vertical walls the h-contribution connected with retention does not deviate much from the prediction in Eqs. (5) and (7). When the vertical walls are also retentive, the f_2 values are about a factor of 2 larger, that is, a factor of 2 is lost in efficiency for strongly retained components.

The separation impedance in pressure drive systems varies strongly with the retention factor, k', as is the case for cylindrical systems. Table 12 compares the SE values for $k' = 4$. As can be seen, the differences in separation impedances are not dramatic. The rectangular system with neglect of edge effects would be slightly better than the open cylindrical column. When the edge effect is taken into account, the cylindrical system is always slightly superior. The system with coating on top and bottom (and not left and right) is the best, those with coating on all walls, or bottom only are worst. With square channels ($\varphi = 1$) the coating scheme does not matter much, except that ''BO'' is unfavourable. Another striking effect is that the SE-values depend less on φ than the plate heights, e.g. the SE values for BT256, B16 and BT1 vary between 20.0 and 21.0, whereas the h values differ much more. This is brought about by the ϕ factor: The better plate height of the BT1 system is offset by the less favourable value for ϕ (28.45 vs. 12.03).

Table 12
Separation impedances for pressure-driven systems

System	ν_{min}	h_{min}	SE
OT	6.5	0.62	12.1
BTNE	5.1	0.79	7.4
BT256	3.0	1.30	21.0
BT16	3.1	1.28	20.4
BT1	4.8	0.84	20.0
BONE	3.6	1.11	14.8
BO256	2.1	1.86	41.7
BO16	2.2	1.80	40.5
BO1	3.4	1.19	40.0
AL256	1.7	2.38	67.9
AL16	1.9	2.15	57.7
AL1	5.0	0.79	17.9

Retention factor $k' = 4$. Codes in first column: ''OT'' = open cylindrical; ''BT'' = coating at bottom and top; ''AL'' = coating at all walls; ''BO'' = coating at bottom wall only; numbers refer to width-to-height ratio, φ; ''NE'' = edge effects neglected (Eqs. (5) and (7)).

References

[1] P. Gebauer, M. Deml, P. Bocek, J. Janak, J. Chromatogr. 267 (1983) 455.
[2] T. Tsuda, J.V. Sweedler, N. Zare, Anal. Chem. 62 (1990) 2149.
[3] A. Manz, E. Verpoorte, H. Ludi, H.M. Widmer, D.J. Harrison, Trac-Trends Anal. Chem. 10 (1991) 144.
[4] P.A. Bristow, J.H. Knox, Chromatographia 10 (1977) 279.
[5] J.H. Knox, M. Saleem, J. Chromatogr. Sci. 7 (1969) 614.
[6] M.J.E. Golay, in: D.H. Desty (Ed.), Gas Chromatography 1958, Butterworths, London, 1958, p. 36.
[7] R. Endele, I. Halasz, K. Unger, J. Chromatogr. 99 (1974) 377.
[8] G. Taylor, Proc. R. Soc. A 219 (1953) 186.
[9] M. van Lieshout, R. Derks, H.G. Janssen, C.A. Cramers, J. High Resolut. Chromatogr. 21 (1998) 583.
[10] H. Poppe, J.C. Kraak, J. Chromatogr. 255 (1983) 395.
[11] R.T. Ghijsen, H. Poppe, J High Resolut. Chromatogr. 11 (1988) 271.
[12] J.H. Knox, M.T. Gilbert, J. Chromatogr. 186 (1979) 405.
[13] R. Swart, J.C. Kraak, H. Poppe, Trends Anal. Chem. 16 (1997) 332.
[14] L.A. Knecht, E.J. Guthrie, J.W. Jorgenson, Anal. Chem. 56 (1984) 479.
[15] R.A. Wallingford, A.G. Ewing, Anal. Chem. 59 (1987) 1762.
[16] N.J. Dovichi, Chem. Br. 24 (1988) 895.
[17] R. Swart, J.W. Elgersma, J.C. Kraak, H. Poppe, J. Microcol. Sep. 9 (1997) 591.
[18] J.C. Giddings, J.P. Chang, M.N. Myers, J.M. Davis, K.D. Caldwell, J. Chromatogr. 255 (1983) 359.
[19] M.J.E. Golay, J. Chromatogr. 216 (1981) 1.
[20] A. Cifuentes, H. Poppe, Chromatographia 39 (1994) 391.
[21] G.E. Spangler, Anal. Chem. 70 (1998) 4805.
[22] C.L. Rice, R. Whitehead, J. Phys. Chem. 69 (1965) 4017.
[23] J.H. Knox, I.H. Grant, Chromatographia 24 (1987) 135.
[24] J.C. Giddings, Dynamics of Chromatography, Part I, Marcel Dekker, New York, 1965.
[25] R. Aris, Proc. Roy. Soc. A 252 (1959) 538.
[26] R. Aris, Proc. Roy. Soc. A 235 (1956) 67.
[27] A.A. Clifford, J. Chromatogr. 471 (1989) 61.
[28] W.H. Press, S.A. Teukolsky, W.T. Vetterling, B.T. Flannery, Numerical Recipes in C, 2nd edition, Cambridge University Press, Cambridge UK, 1992.
[29] E. Chmela, M.T. Blom, J.G.E. Gardeniers, A. van den Berg, R. Tijssen, In: Proceedings μTAS'01 Conference, J.M. Ramsey, A. van den Berg (Eds.), Kluwer Academic Publishers, Dordrecht 2001, pp. 646–648.
[30] S.C. Jacobson, T.E. McKnight, B.S. Broyles, J.P. Alarie, C.T. Culbertson, J.M. Ramsey, Presented at the International Symposium on High-Performance Liquid Phase Separations and Related Techniques, Kyoto, 11–14 September 2001, lecture L 59.